九州大学大学院総合理工学報告
第 46 巻 第 1 号 7-18 頁 令和 6 年 9 月

Engineering Sciences Reports, Kyushu University
Vol. 46, No. 1, pp. 7-18, SEP, 2024

Rovibrational Distribution of CS($A^1\Pi$) Produced by Collisions of Metastable Kr($^3P_2$) Atoms with CS_2 in the Flowing Afterglow

Masaharu TSUJI,[*1,2†] Masafumi NAKAMURA,[*3]
Nobuo KANEKO[*3] and Hiroshi OBASE[*4]
[†]E-mail of corresponding author: tsuji@cm.kyushu-u.ac.jp

(Received March 5, 2024, accepted March 13, 2024)

Rovibrational distribution of CS($A^1\Pi$) produced by the Kr($^3P_2$)/CS_2 reaction was studied by observing CS($A^1\Pi$–$X^1\Sigma^+$) emission in the flowing afterglow. The CS(A–X) emission from v'= 0–5 was identified in the 245–275 nm region. The band intensities from the CS(A:v'= 1–4) levels were combined with calculated RKR Franck-Condon factors (FCFs) to analyze the dependence of the electronic transition moment on r-centroid. The relative vibrational formation rates of CS(A:v'= 0–5), $P_{v'}$, were estimated to be 1.00:0.94:0.65:0.41:0.19:0.08. The rotational distributions of CS(A:v'= 0–5) were expressed by single Boltzmann rotational temperatures (T_R) of 2300, 2000, 1800, 1500, 1400, and 1200 K, respectively. From the observed $P_{v'}$ and T_R data, the average fractions of excess energy deposited into vibrational and rotational energies of CS(A), and relative translational energy of products were determined to be $<f_v>$=25%, $<f_r>$=24%, and $<f_t>$=51%, respectively. The observed $P_{v'}$ and T_R data of CS(A:v'= 0–5) were compared with previous data for the Ar($^3P_2$)/CS_2 reaction and vacuum ultraviolet (VUV) photoexcitation. They were also compared with statistical prior vibrational and rotational distributions to examine the reaction dynamics. Possible precursor Rydberg states of CS_2** in the Kr($^3P_2$)/CS_2 and Ar($^3P_2$)/CS_2 reactions were discussed from reported fluorescence cross section data.

Key words: *Flowing afterglow, Metastable Kr($^3P_2$) atom, CS_2, Energy transfer, Dissociative excitation, CS(A-X) emission, Electronic transition moment, Rovibrational distribution, Rotational temperature, Prior distribution, Rydberg state*

1. Introduction

Optical spectroscopic studies on energy transfer reactions between rare gas metastable atoms and CS_2 have been extensively studied for He(2^3S:19.82 eV), Ne($^3P_2$:16.62 eV and $^3P_0$:16.72 eV), Ar($^3P_2$:11.55 eV and $^3P_0$:11.72 eV), and Xe($^3P_2$:8.32 eV and $^3P_0$:9.45 eV) atoms.[1-10] In the reactions of He* and Ne* atoms with higher excitation energy than the ionization potentials of CS_2^+($\tilde{X}\,^2\Pi_g$:10.07 eV, $\tilde{A}\,^2\Pi_u$:12.7 eV, $\tilde{B}\,^2\Sigma_u^+$:14.48 eV), major emitting product channels are Penning ionization leading to excited CS_2^+($\tilde{A}^2\Pi_u$, $\tilde{B}^2\Sigma^+$) states:[1-5]

*1 Institute for Materials Chemistry and Engineering, and Research and Education Center of Green Technology
*2 Department of Molecular Science and Technology
*3 Department of Molecular Science and Technology, Graduate Student
*4 Research Institute of Industrial Science, Kyushu University

$$He(2^3S) + CS_2 \rightarrow CS_2^+(\tilde{A}^2\Pi_u, \tilde{B}^2\Sigma_u^+) + He + e^-, \quad (1)$$

$$Ne(^3P_{2,0}) + CS_2 \rightarrow CS_2^+(\tilde{A}^2\Pi_u, \tilde{B}^2\Sigma_u^+) + Ne + e^-. \quad (2)$$

In the He and Ne afterglow reaction of CS_2, besides the above Penning ionization processes, the following electron-ion recombination process leading to excited CS($A^1\Pi$,$a^3\Pi$) states have been observed:[1-3,8]

$$CS_2^+ + e^- \rightarrow CS(A^1\Pi, a^3\Pi) + S \quad (3)$$

Here, CS_2^+ ions and electrons are dominantly formed by He(2^3S)/CS_2 and Ne($^3P_{2,0}$)/CS_2 Penning ionization such as processes (1) and (2). Molek et al.[11] determined vibrational distributions of CS($A^1\Pi$:v'= 0–4, $a^3\Pi$:v'= 0–2) in process (3) by using a flowing afterglow (FA) method.

In the Ar* and Xe* reactions with lower excitation energy than the ionization potential of CS_2^+($\tilde{A}$), major emitting product channels

are the formation of CS($A^1\Pi$) and/or CS($a^3\Pi$) by dissociative excitation, respectively:[6-10]

$$Ar(^3P_{2,0}) + CS_2 \rightarrow CS(A^1\Pi, a^3\Pi) + S + Ar, \quad (4)$$
$$Xe(^3P_{2,0}) + CS_2 \rightarrow CS(a^3\Pi) + S + Xe. \quad (5)$$

The vibrational distribution of CS(A) in process (4) has been determined by Marcoux et al.,[8] Wu,[9] and Xu et al.[10] Marcoux et al.[8] determined the vibrational population of CS(A: $v' = 0-5$) in the Ar FA. They also measured the dependence of vibrational distribution of CS(A:$v'= 0-5$) in process (3) on the He buffer gas pressure in the He FA to examine vibrational relaxation by collisions with the He gas. Wu[9] observed CS(A–X) emission in the Ar FA. He noticed that besides the Ar($^3P_2$)/CS_2 reaction, CS_2^+/e^- recombination reaction (3) may participate in the formation of CS(A), because major output channel (74±17%) of the Ar($^3P_2$)/CS_2 reaction is Penning ionization:[12]

$$Ar(^3P_2) + CS_2 \rightarrow CS_2^+(\tilde{X}) + Ar + e^-, \quad (6).$$

where precursor CS_2^+ and e^- are formed simultaneously. No effects of SF_6 addition as a typical electron scavenger led him to conclude that electron-ion recombination process (3) was insignificant in their condition. It was therefore concluded that CS(A–X) emission results exclusively from the Ar($^3P_2$)/CS_2 reaction (4). Wu determined the relative vibrational formation rate of CS(A:$v'= 0-5$), $P_{v'}$, in the Ar($^3P_2$)/CS_2 reaction using the relation,

$$(P_{v'}/P_{v'=0}) = (N_{v'}/N_{v'=0})\,(\tau_{v'=0}/\tau_{v'}), \quad (7)$$

where $N_{v'}$ is steady-state vibrational population and $\tau_{v'}$ is the radiative lifetime of v' level measured by Carlson et al.[13] Since the $\tau_{v'}$ value increases from 185 ns to 225, 220, 230, 235, and 255 ns with increasing the vibrational level from $v'= 0$ to $v'= 1-5$, respectively,[13] $P_{v'}$ values for $v' = 1-5$ are smaller than corresponding $N_{v'}$ values by 18–27%. Although Wu did not compare his $N_{v'}$ distribution with previous pioneering data of Marcoux et al.[8] measured in the same Ar FA, it was much lower than that of Marcoux et al.[8] Xu et al.[10] measured rovibrational distribution of CS(A) in the Ar($^3P_2$)/CS_2 reaction using FA coupled with a low-pressure chamber. The observed $P_{v'}$ distribution was more excited than that of Wu.[7] They attributed high vibrational excitation in their low-pressure experiment to the great reduction of vibrational relaxation of CS(A:$v'= 1-5$) by collision with buffer Ar gas. The rotational distribution decreased with an increase in v' from 10000± 300 K for $v'= 0$ to 5600±300 K for $v'= 5$. Xu et al.[10] did not compare their vibrational distribution with the $N_{v'}$ distribution of Marcoux et al.[8] When the $P_{v'}$ distribution of Marcoux et al. was calculated using Eq. (7), difference in the $P_{v'}$ distribution between the two experiments was small.

Dissociative excitation pathways of CS_2 by the Ar($^3P_2$)/CS_2 reaction leading to CS(A) has been discussed by Wu[9] and Xu et al.[10] Wu reported that CS(A) originates from predissociation of the Rydberg state converging into the ground state of CS_2^+ below the ionization limit, via a very steep repulsive potential curve. He concluded that a significant amount of excess energy is deposited into translational energy because of low vibrational excitation of CS(A). Although Xu et al.[10] reported that CS(A) is formed via at least five steps E-E transfer involving Rydberg state, possible Rydberg states were not discussed.

Coxon et al.[1] observed CS(A–X) emission in the He afterglow reaction of CS_2 and determined the dependence of electronic transition moment on the r-centroid from the intensity distributions of $v' = 0-4$ v''-progressions. However, there was a large variation in their data with respect to the fitting line.

Although optical spectroscopic studies on energy-transfer reactions of He*, Ne*, Ar*, and Xe* atoms with CS_2 have been carried out, that of Kr* has not been reported to our best knowledge. The total reaction rate constant of the Kr($^3P_2$)/CS_2 reaction has been measured as 8.0×10^{-10} cm^3s^{-1} at 300 K by using an FA technique.[14] This value is smaller than that for the Ar($^3P_2$)/CS_2 reaction by 25% (1.06×10^{-9} cm^3s^{-1}).[14]

VUV photolysis of CS_2 has been studied by Lee and Judge[15] and Ashhold et. al.[16] Lee and Judge observed CS(A–X) emission by VUV photons in the 123.9–68.6 nm (10.01–18.07 eV) region and determined $N_{v'}$ distributions at 92.3 nm (13.43 eV) and 123.9 nm (10.01 eV). Ashfold et al. measured CS(A–X) emission by VUV photons in the 130.4–121.6 nm (9.51–10.20 eV) range under better optical resolution than that of Lee and Judge. They determined the dependence of $N_{v'}$ distribution on the excitation wavelength. The rotational temperature of CS(A:$v'=0$) under 130.4 nm (9.51 eV) excitation was determined from a spectral simulation.

In the present study, the energy-transfer reaction of metastable Kr($^3P_2$:9.92 eV) atoms with CS_2 is investigated by observing CS(A–X) emission in the FA. The dependence of electronic transition moment on r-centroid is determined from the intensity distribution of v'=0–4 v''-progressions of CS(A–X) emission, where overlapping with higher v' v''-progressions can be reduced greatly. The vibrational and rotational populations of CS(A: v' = 0–5) are determined. The $P_{v'}$ distribution is estimated from Eq. (7). The $N_{v'}$ and $P_{v'}$ data obtained in this study are compared with the reported $N_{v'}$ and $P_{v'}$ data in the Ar($^3P_2$)/CS_2 reaction[8-10] and $N_{v'}$ data in VUV photoexcitation with similar energies (123.6 nm = 10.03 eV).[16] The observed rovibrational distributions are also compared with statistical prior ones to obtain information on the reaction dynamics. Possible precursor CS_2** Rydberg states leading to CS(A) in the Kr($^3P_2$)/CS_2 and Ar($^3P_2$)/CS_2 reactions are discussed based on reported fluorescence excitation spectra and cross section data in the VUV region.[17,18]

2. Experimental

The FA apparatus was identical with that used for the Kr($^3P_2$)/CO reactions.[19] In brief, argon gas (>purity 99.999%) was excited to the metastable $^3P_{2,0}$ states by a microwave discharge operated at an Ar buffer gas pressure of about 0.1 Torr (1 Torr= 133.3 Pa). The metastable Kr($^3P_2$) atoms were generated by adding a small amount of Kr(> 99.995%:5–20 mTorr) gas to the Ar flow prior to the discharge. CS_2 was added from an orifice placed 10 cm downstream from the center of microwave discharge. The partial pressure of CS_2 in the reaction zone was a few mTorr.

The emission spectra were observed with a 1 m monochromator (Jarrell Ash M2) equipped with a 1200 grooves/mm grating, blazed at 300 nm. The spectral response curve of the monochromator with a Hamamatsu Photonics R376 photomultiplier was calibrated by using a standard halogen lamp.

3. Results and discussion

3.1 CS(A-X) emission from the Kr($^3P_2$)/CS_2 reaction and the dependence of electronic transition moment on r-centroid

Figure 1a shows a typical emission spectrum obtained from the Kr($^3P_2$)/CS_2 reaction, where the CS($A^1\Pi$–$X^1\Sigma^+$) emission system from v' = 0–5 vibrational levels is identified. Emissions from $\Delta v'$= 1, 0, and -1 sequences are much stronger than those of $\Delta v'$ = 2 sequence due to low vibrational excitation above v' = 3. For comparison, CS(A–X)

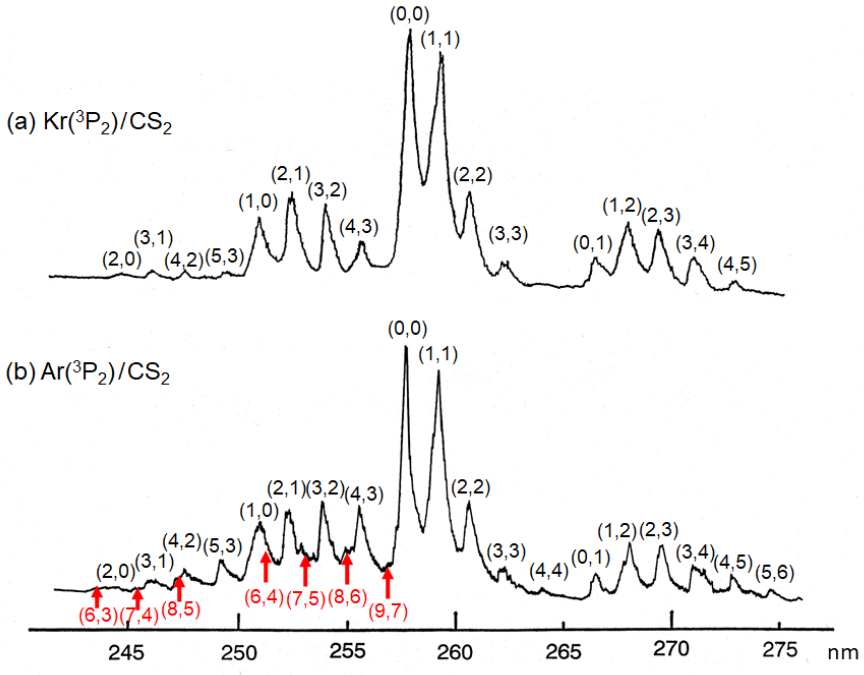

Fig. 1. Emission spectra of CS(A–X) produced from the (a) Kr($^3P_2$)/CS_2 and (b) Ar($^3P_2$)/CS_2 reactions.

emission produced from the $Ar(^3P_2)/CS_2$ reaction is shown in Fig. 1b. Although the same CS(A–X) emission from $v' = 0–5$ levels is observed as reported previously,[8-10] spectral features are different from those in the $Kr(^3P_2)/CS_2$ reaction. In the case of the $Ar(^3P_2)/CS_2$ reaction, CS(A) radicals are more vibrationally excited, so that progressions from high v' levels are partially overlapped with those from low v' levels. For example, weak (6,3), (7,4), and (8,5) bands appear on the blue side of the (2,0), (3,1), and (4,2) bands, and weak (6,4), (7,5), (8,6), and (9,7) bands are observed on the red side of the (1,0), (2,1), (3.2), and (4,3) bands, respectively, as shown in red color in Fig. 1b. Therefore, precise measurements of relative intensities of each band are difficult without spectral simulation. On the other hand, CS(A–X) emission from high v' levels in the $Kr(^3P_2)/CS_2$ reaction is much weaker than that in the $Ar(^3P_2)/CS_2$ reaction. Therefore, more reliable intensity distribution of CS(A–X) emission from low vibrational levels can be obtained in the $Kr(^3P_2)/CS_2$ reaction.

In general, the band intensity (photons s^{-1}) of a transition from a (v',J') level to a $(v",J")$ level is expressed as

$$I_{v'J'v"J"} \propto N_{v'J'}\, Re^2(\bar{r}_{v'v"}) q_{v'v"} \nu^3_{v'J'v"J"} S_{J'J"}/g_{J'}, \quad (8)$$

where $N_{v'J'}$ is the rotational population in a given vibrational level v', $Re(\bar{r}_{v'v"})$ the electronic transition moment, $q_{v'v"}$ the FCF, $\nu_{v'J'v"J"}$ the transition frequency, $S_{J'J"}$ the rotational line strength, and $g_{J'} = 2J' + 1$.[20]

The dependence of electronic transition moment on r-centroid, $Re(\bar{r}_{v'v"})$, is obtained from the relation for a $(v', v")$ band:

$$Re(\bar{r}_{v'v"}) \propto [I_{v'v"}/q_{v'v"}\nu^3_{v'v"}]^{1/2} \quad (9)$$

Data from individual $v"$-progressions are scaled by Fraser's method[21] to account for the different populations among the upper state vibrational levels. Coxon et al.[1] determined the $Re(\bar{r}_{v'v"})$ function from the intensity distributions of $v' = 0–4$ $v"$-progressions of CS(A–X) emission in the He afterglow. CS(A) radicals resulting from the CS_2^+/e^- recombination reaction (3) in the He afterglow are more vibrationally excited than that in the $Kr(^3P_2)/CS_2$ reaction, as in the case of the $Ar(^3P_2)/CS_2$ reaction. Therefore, there was a large variation in their data with respect to the fitting line probably due to heavy overlapping of high v' $v"$-progressions with low v' $v"$-progressions. In addition, their RKR FCF and r-centroid values were calculated using old spectroscopic data.[22] These provide large uncertainty in the estimation of $Re(\bar{r}_{v'v"})$ values for transitions with small FCFs.

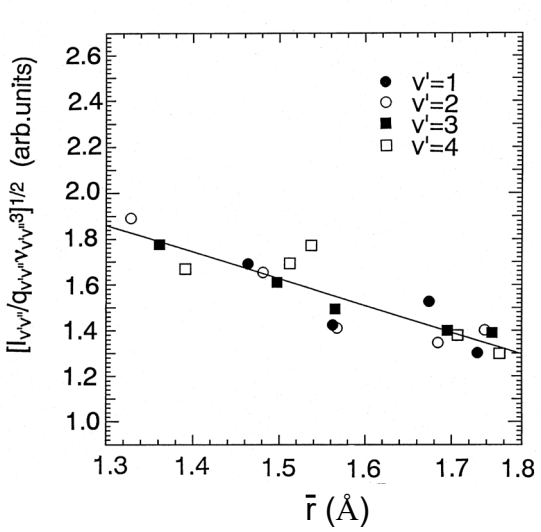

Fig. 2. Dependence of electronic transition moment of the CS(A–X) transition on r-centroid.

We calculated RKR FCFs and r-centroids using more reliable spectroscopic data reported by Bergeman and Cossart.[23] Results obtained were in reasonable agreement with their reported data calculated using RKR potentials.[23] Figure 2 shows the dependence of electronic transition moment on r-centroid, obtained from $v' = 1–4$ $v"$-progressions of CS(A–X) emission in the $Kr(^3P_2)/CS_2$ reaction. It should be noted that variation in our data with respect to the fitting line is greatly reduced in comparison with the previous data of Coxon et al.[1] The following linear fitting curve was obtained:

$$Re(\bar{r}_{v'v"}) = C(1 - 0.35\bar{r}_{v'v"}). \quad (10)$$

The slope of Eq. (10) is slightly smaller than 0.40 reported by Coxon et al.[1] It is much smaller than 0.465 obtained by Mahon et al.[24] from laser-induced fluorescence measurements. We used Eq. (10) for the estimation of $Re(\bar{r}_{v'v"})$ values in Eq. (8).

3.2 Rovibrational distribution of CS(A) produced from the $Kr(^3P_2)/CS_2$ reaction

Rovibrational distribution of CS(A) in the $Kr(^3P_2)/CS_2$ reaction was determined by a computer simulation of emission spectrum

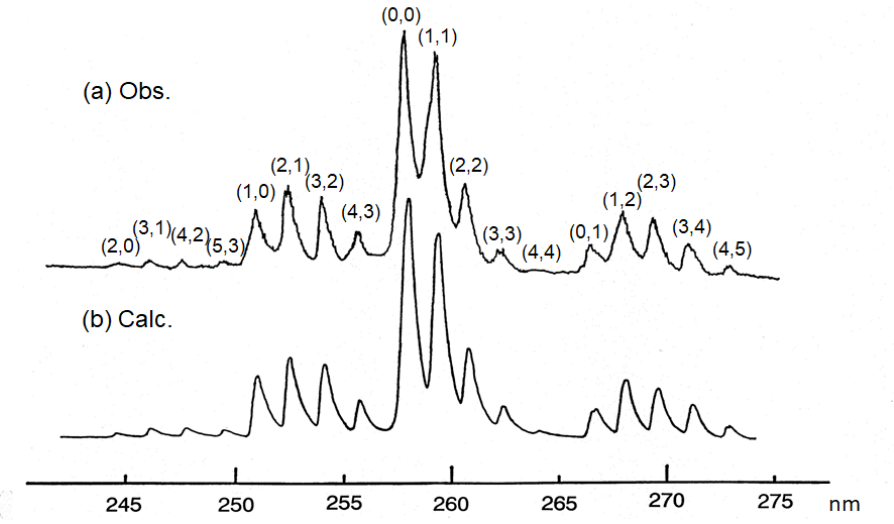

Fig. 3. (a) observed and (b) simulated emission spectra of CS(A−X) produced from the Kr($^3P_2$)/CS_2 reaction.

because rotational structure was not resolved in the present optical resolution. The rotational line strength $S_{J'J''}$ in Eq. (8) was deduced from the formula given by Kovács.[25] A Gaussian slit function was convoluted into rotational lines to calculate the spectral envelope.

Richards and Setser[26] studied the formation of CS($A^1\Pi$,$a^3\Pi$) by the $N_2(A^3\Sigma_u^+)$/CS reaction in the Ar FA and found that variation of the Ar pressure from 1.9 to 8 Torr showed no significant change in the CS(A−X) spectrum. Therefore, they concluded that collisional relaxation by collisions with buffer Ar gas within radiative lifetimes of 185−255 ns is insignificant and vibrational distribution of CS(A) obtained at an Ar pressure of 2.9 Torr can be taken as the nascent distribution. In the present experiment, Ar gas pressure was 0.1 Torr, which was much lower than their experiment. It was therefore concluded that rovibrational distribution of CS(A) obtained from the Kr($^3P_2$)/CS_2 reaction in this study reflects nascent distribution.

In Figs. 3a and 3b are shown the observed and best fit spectra of the CS(A−X) band obtained assuming single Boltzmann rotational distributions for each v' level. The $N_{v'}$ values and rotational temperatures of CS(A:v'= 0−5) in the Kr($^3P_2$)/CS_2 reaction obtained from spectral simulation are given in Table 1 together with corresponding $P_{v'}$ values evaluated from Eq. (7). In Table 1, the most

Table 1. Vibrational population, relative vibrational formation rate, and rotational temperatures of CS(A:v'=0−6) produced from the Kr($^3P_2$)/CS_2 and Ar($^3P_2$)/CS_2 reactions and VUV photoexciation at 123.6 nm (10.03 eV). Two-body and three-body prior distributions in the Kr($^3P_2$)/CS_2 reaction are also shown.

	Kr($^3P_2$) 9.92 eV This work					Ar($^3P_2$) 11.55 eV Ref. 10			VUV 10.03 eV Ref. 16	
v'	$N_{v'}$	$P_{v'}$	$P^o_{v'}$ Two-body	$P^o_{v'}$ Three-body	T_R/K	$N_{v'}$	$P_{v'}$	T_R/K	$N_{v'}$	$P_{v'}$
v'=0	1.00	1.00	1.00	1.00	2300	1.00	1.00	10000±300	1.00	1.00
v'=1	1.14	0.94	0.74	0.54	2000	1.69	1.39	9000±300	0.79	0.65
v'=2	0.77	0.65	0.51	0.26	1800	1.26	1.06	8100±300	0.63	0.53
v'=3	0.51	0.41	0.31	0.10	1500	0.63	0.51	7200±300	0.49	0.39
v'=4	0.24	0.19	0.15	0.023	1400	0.50	0.39	6400±300	0.43	0.34
v'=5	0.11	0.08	0.04	0.002	1200	0.44	0.32	5600±30	0.26	0.19
v'=6									0.10	

reliable $N_{v'}$ and $P_{v'}$ data for the Ar($^3P_2$)/CS_2 reaction[10] and VUV excitation at 123.6 nm[16] are also given for comparison. In the VUV excitation, $N_{v'}$ values were measured for the v'= 0–6 levels. To the best of our knowledge, radiative lifetime of v'= 6 has not been known, so that only $N_{v'}$ value is shown for VUV data.

Figure 4 shows $P_{v'}$ distributions in the Kr($^3P_2$)/CS_2 and Ar($^3P_2$)/CS_2 reactions and VUV excitation at 123.6 nm. Results shown in Table 1 and Fig. 4 indicate that CS(A) in the Kr($^3P_2$) reaction is less vibrationally excited than that in the Ar($^3P_2$) reaction. The rotational temperatures of CS(A) in the Kr($^3P_2$) reaction are lower those in the Ar($^3P_2$) reaction by factors of 4.3–4.8. The vibrational distribution of CS(A:v' = 1–3) in the Kr($^3P_2$) reaction is higher than that of VUV excitation at 10.03 eV, whereas that of CS(A:v'= 4,5) in the Kr($^3P_2$) reaction is lower than the VUV distribution. The difference between the Kr($^3P_2$) reaction and VUV excitation with a similar excitation energy is smaller than that between the Kr($^3P_2$) and Ar($^3P_2$) reactions.

Total available energies, E_{tot}, given in Table 2, were estimated from the relation ΔH_0^o + (5/2)RT at 300 K for the reactions:

$$Kr(^3P_2) + CS_2 \rightarrow CS(A{:}v'{=}0) + S(^3P_2) + 0.65\ eV \quad (11)$$

$$Ar(^3P_2) + CS_2 \rightarrow CS(A{:}v'{=}0) + S(^3P_2) + 2.28\ eV \quad (12)$$

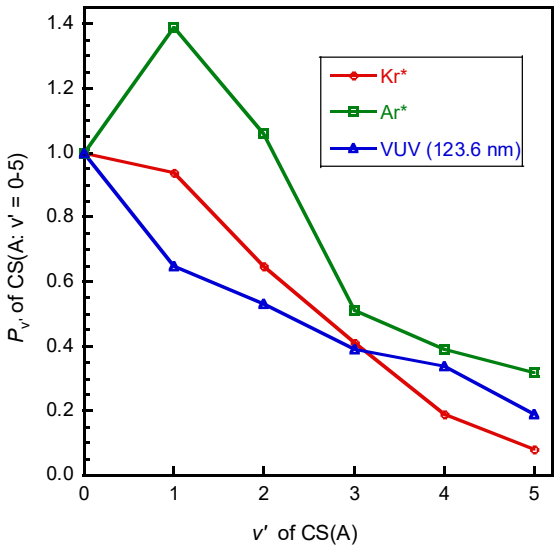

Fig. 4. Vibrational distribution of CS(A) produced by Kr($^3P_2$), Ar($^3P_2$),[10] and VUV photoexcitation (123.6 nm).[16]

On the other hand, the E_{tot} value in VUV photodissociation (13) was obtained from the relation ΔH_0^o + RT at 300 K.

$$h\nu\ (123.6\ nm{:}\ 10.03\ eV) + CS_2 \rightarrow CS(A{:}v'{=}0) + S(^3P_2) + 0.76\ eV \quad (13)$$

In the evaluation of ΔH_0^o values, the dissociation energy of D(CS–S)=4.463 eV and excitation energy of CS(X:v''=0→A:v'=0)=4.81 eV were obtained from reported data.[17,27] The E_{tot} value of the Kr($^3P_2$) reaction is decreased to about 1/3 in comparison with that of the Ar($^3P_2$) reaction. This will be a major reason for the lower vibrational and rotational excitation in the Kr($^3P_2$) reaction than that in the Ar($^3P_2$) reaction. On the other hand, difference in the E_{tot} value between the Kr($^3P_2$) reaction and VUV excitation is small (0.07 eV). This small difference will be a major reason for the small difference in the vibrational distribution between the two excitation methods.

From the observed rovibrational distributions of CS(A) and E_{tot} value, we estimated the average vibrational and rotational energies of CS(A), denoted as $<E_v>$ and $<E_r>$, and the average yields of total available energy into these degrees of freedom, denoted as $<f_v>$ and $<f_r>$, respectively from the relations:

$$<E_v> = \sum_{v'} P_{v'} E_{v'} / \sum_{v'} E_{v'}, \quad (14)$$

$$<f_v> = <E_v>/E_{tot}, \quad (15)$$

$$<E_r> = k \sum_{v'} P_{v'} T_{v'} / \sum_{v'} P_{v'}, \quad (16)$$

$$<f_r> = <E_r>/E_{tot}. \quad (17)$$

From the $<E_v>$ + $<E_r>$ value, the average relative translational energy of CS(A) + S and its fraction to total available energy, $<E_t>$ and $<f_t>$, respectively, were evaluated from the relations:

$$<E_t> = E_{tot} - (<E_v> + <E_r>), \quad (18)$$

$$<f_t> = <E_t>/E_{tot}. \quad (19)$$

The $<E_v>$, $<E_r>$, $<E_t>$, $<f_v>$, $<f_r>$, and $<f_t>$ values thus obtained for the Kr($^3P_2$) reaction are summarized in Table 2 along with the reported data of the Ar($^3P_2$) reaction and VUV photoexcitation (10.03 eV). For VUV excitation, only $<E_v>$ and $<f_v>$ values obtained from $P_{v'}$ (v' = 0–5) values are shown because rotational distributions of each vibrational state were not determined. The $<f_v>$ value of the Kr($^3P_2$) reaction is 2.7 times larger than

that of the Ar($^3P_2$) reaction, whereas the $<f_r>$ value of the Kr($^3P_2$) reaction is 23% smaller than that of the Ar($^3P_2$) reaction. The $<f_v>$ + $<f_r>$ value of the Kr($^3P_2$) reaction is 21% larger than that of the Ar($^3P_2$) reaction. This result indicates that deposition of excess energy into internal energy is more favorable in the Kr($^3P_2$) reaction, whereas that into translational energy is more favorable in the Ar($^3P_2$) reaction. The $<f_v>$ value in the Kr($^3P_2$) reaction was comparable with that in VUV excitation.

Table 2. Average vibrational and rotational energies deposited into CS(A) and relative translational energy deposited into CS(A) + S, and average fractions of above energies to total available energies in the Kr($^3P_2$)/CS_2 and Ar($^3P_2$)/CS_2 reactions and VUV (10.03 eV) photoexcitation.

	Kr($^3P_2$)	Ar($^3P_2$)	VUV 123.6 nm
	This work	Ref. 10	Ref. 16
E_{tot} (eV)	0.71 eV	2.34 eV	0.78 eV
$<E_v>$	0.18 eV	0.22 eV	0.21 eV
$<E_r>$	0.17 eV	0.72 eV	
$<E_t>$	0.36 eV	1.40 eV	
$<f_v>$	25%	9.4%	27%
$<f_r>$	24%	31%	
$<f_t>$	51%	60%	

3.2 The reaction dynamics for the formation of CS(A) in the Kr($^3P_2$)/CS_2 reaction

3.2.1 Statistical models

The formation dynamics of CS(A) from the Kr($^3P_2$)/CS_2 reaction is discussed assuming two-body and three-body dissociation mechanisms, which have been used in the formation of OH($A^2\Sigma^+$) from the Ar($^3P_{0,2}$)/H_2O reaction.[28]

(a) Two-body dissociation process through resonant excitation transfer:

$$Kr^* + CS_2 \rightarrow CS_2^* + Kr,$$
$$CS_2^* \rightarrow CS(A) + S, \quad (20)$$

(b) Two-body dissociation process through ion-pair intermediate:

$$Kr^* + CS_2 \rightarrow Kr^+CS_2^- \rightarrow KrCS^* + S,$$
$$KrCS^* \rightarrow CS(A) + Kr, \quad (21)$$

(c) Three-body dissociation process through resonant excitation transfer:

$$Kr^* + CS_2 \rightarrow KrCS_2^*,$$
$$KrCS_2^* \rightarrow CS(A) + S + Kr. \quad (22)$$

In processes (a), energy is resonantly transferred from Kr* to CS_2, and then CS_2* dissociates into CS(A) + S. In process (b) KrCS* intermediate is formed through $Kr^+CS_2^-$ ion pair. In process (c), CS(A) radicals are produced through three-body dissociation of $KrCS_2$* complex. The electron affinity of CS_2 has been measured as 0.5525±0.0013 eV,[29] so that stable CS_2^- anion can be formed. Whereas the neutral $CS_2(X^1\Sigma_g^+)$ molecule is linear, the corresponding anion, $CS_2^-(X^2A_1)$, is bent ∠SCS ≈145°,[30,31] leading to poor FC overlap in the vertical $CS_2(X^1\Sigma_g^+) \rightarrow CS_2^-(X^2A_1)$ electron attachment process. Thus transfer from entrance $V(Kr^*, CS_2)$ potential to $V(Kr^+, CS_2^-)$ ion-pair one will be inefficient. We therefore excluded process (b) through $Kr^+CS_2^-$ ion-pair complex from the above three possible reaction processes.

Statistical vibrational and rotational distributions were calculated for two processes (a) and (c). According to a simple statistical theory,[32-35] the probability of forming a CS $(A: v', J')$ rovibrational level through processes (a) and (c) is, respectively, expressed by

$$P^o_{v'J'} \propto (2J'+1)\left(E_{\rm tot} - E_{v_{CS^*}}\right)^{1/2}, \quad (23a)$$

$$P^o_{v'} \propto \left(E_{\rm tot} - E_{v_{CS^*}}\right)^{3/2}, \quad (23b)$$

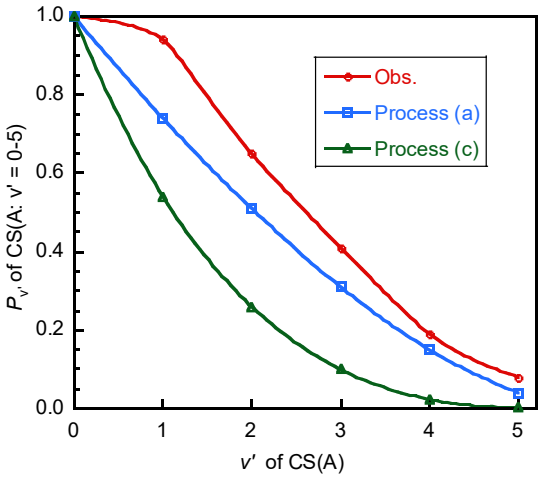

Fig. 5. Observed and two-body and three-body prior vibrational distributions in the Kr($^3P_2$)/CS_2 reaction.

$$P^o_{v'J'} \propto (2J'+1)\left(E_{\rm tot} - E_{v_{\rm CS}*}\right)^2, \quad (24a)$$

$$P^o_{v'} \propto \left(E_{\rm tot} - E_{v_{\rm CS}*}\right)^3. \quad (24b)$$

The prior vibrational and rotational distributions of CS(A: v'=0–5) for processes (a) and (c) are compared with the observed ones in Figs. 5 and 6a–6f, and Table 1. Both two-body and three-body prior vibrational distributions of CS(A: v' =0–5) predict lower distributions than observed one. The observed rotational temperature decreases from 2300 K to 1200 K with increasing v' from 0 to 5. Therefore, peak population slowly decreases from J'=32 to 30, 28, 26, 25, and 23 with increasing v' from 0 to 5, respectively. Peaks of two-body and three-

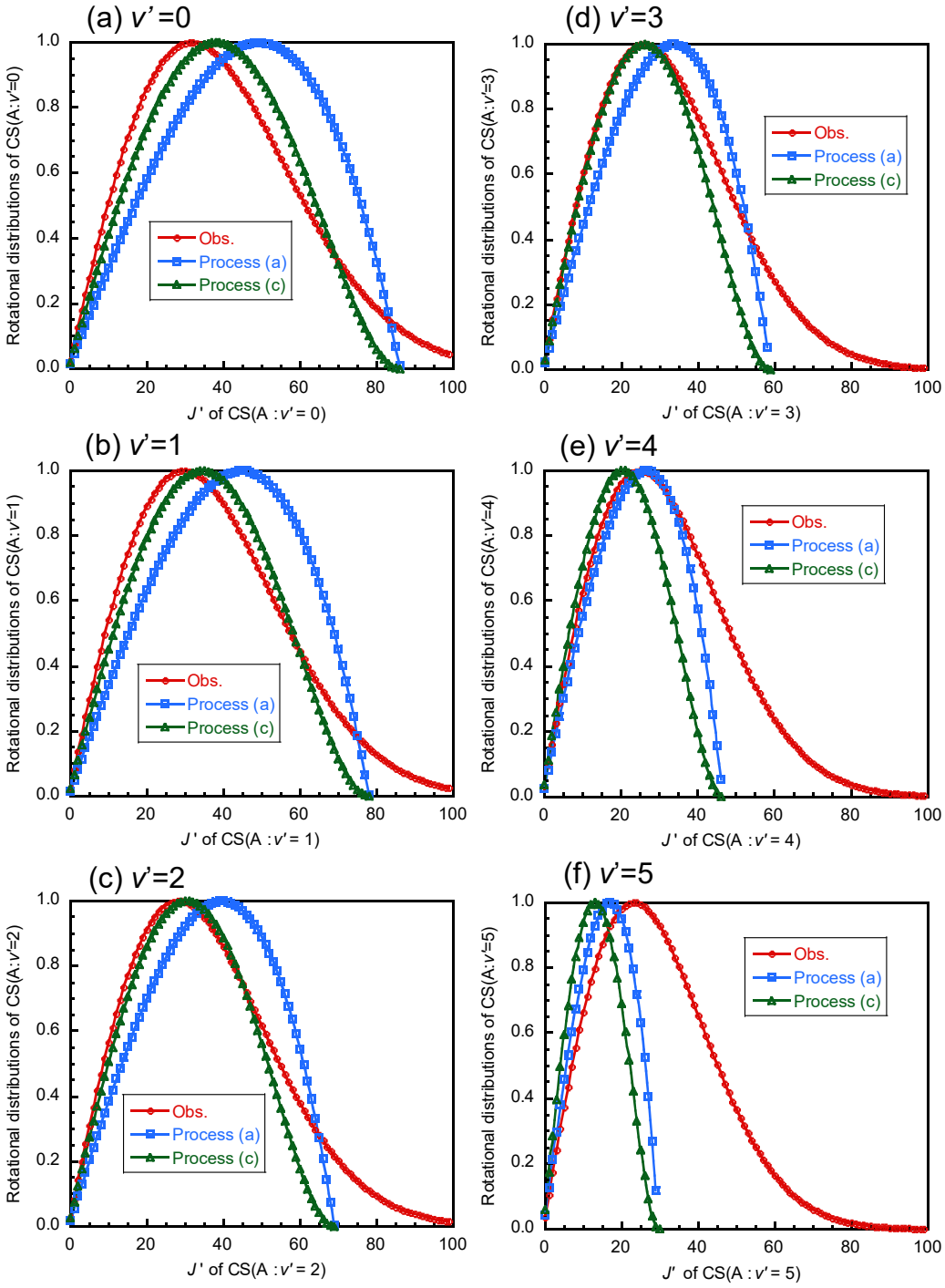

Fig. 6. Observed and statistical prior rotational distributions of CS(A: v' =0–5) in the Kr($^3P_2$)/CS_2 reaction.

body prior rotational distributions decrease more rapidly from J'=49 and 38 for v'=0 to J'=45 and 34 for v'=1, J'=40 and 30 for v'=2, J'=34 and 26 for v'=3, J'=27 and 20 for v'=4, and J'=17 and 13 for v'=5, respectively. These results indicate that observed vibrational and rotational distributions cannot be explained by two- and three-body statistical prior models. On the basis of above findings, CS(A) radicals are not formed via long lived intermediates where excess energy is distributed statistically before predissociation.

3.2.2 Dissociation pathways

Based on extensive experimental studies on energy-transfer reactions from metastable Ar($^3P_2$), Kr($^3P_2$), Xe($^3P_2$) atoms to such diatomic molecules as N_2 and CO, the formation of near-resonant states via E-E transfer is major exit channel in most cases, because conversion of internal energy of metastable atoms to relative translational energy of products (E-T transfer) is unfavorable.[19.36-50] It is therefore reasonable to assume that CS($A^1\Pi$) + S($^3P_2$) products result from near-resonant E-E transfer followed by predissociation of CS_2** states in the Kr($^3P_2$)/CS_2 and Ar($^3P_2$)/CS_2 reactions.

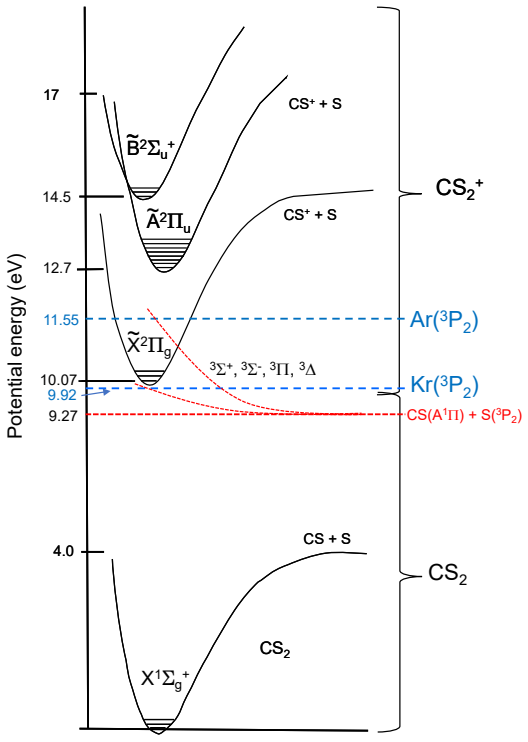

Fig. 7. Potential energy curves of bound $CS_2(X^1\Sigma_g^+)$ and $CS_2^+(\tilde{X}\,^2\Pi_g,\ \tilde{A}\,^2\Pi_u,\ \tilde{B}\,^2\Sigma_u^+)$ states and repulsive CS($A^1\Pi$) + S($^3P_2$) states and energies of Ar($^3P_2$) and Kr($^3P_2$).

Figure 7 shows potential energy diagram of $CS_2(X^1\Sigma_g^+)$, $CS_2^+(\tilde{X}^2\Pi_g,\ \tilde{A}^2\Pi_u,\ \tilde{B}^2\Sigma_u^+)$, repulsive CS($A^1\Pi$) + S($^3P_2$) potentials, and Kr($^3P_2$) and Ar($^3P_2$) atoms. From the correlation diagram, high-energy $^3\Sigma^+$, $^3\Sigma^-$, $^3\Pi$, and $^3\Delta$ states of CS_2* arise from the CS($A^1\Pi$) + S(^3P) dissociation limit.[51] It should be noted that the CS($A^1\Pi$) + S($^3P_2$) dissociation limit is only 0.65 eV below the energy of Kr($^3P_2$), and the energy of Kr($^3P_2$) is 0.15 eV below the ground $CS_2^+(\tilde{X})$ ionic state. Since no ionic states can be formed in the Kr($^3P_2$)/CS_2 reaction, only high-energy neutral states can be precursor states of CS($A^1\Pi$) + S($^3P_2$) fragments. In the Ar($^3P_2$)/CS_2 reaction, the energy of Ar($^3P_2$) is 1.48 eV higher than the $CS_2^+(\tilde{X})$ state, so that the CS($A^1\Pi$) + S($^3P_2$) fragments are expected to be formed via near-resonant superexcited CS_2** states.[52]

Since spin-orbit interaction by the presence of two heavy S atoms is large for CS_2, intersystem crossing between singlet and triplet states will occur efficiently. Therefore, CS($A^1\Pi$) + S($^3P_2$) fragments, which correlate with triplet CS_2* states, are formed under VUV photoexciation.[15-18] This indicates that spin-conservation rule is violated for CS_2 under photoexcitation. The violation of spin-conservation rule is expected to be held in the Rg($^3P_2$) (Rg=Kr, Ar) excitation, where triplet states are favored according to this rule. Both singlet and triplet states can be formed under VUV and Rg($^3P_2$) excitation. It is therefore reasonable to discuss possible precursor CS_2** states in the Rg($^3P_2$) excitation from reported VUV absorption, fluorescence cross-section, and fluorescence quantum yield data of CS_2.[17,18] Okabe[17] measured absorption and CS(A–X) fluorescence excitation spectra of CS_2 in the 120–135 nm region. In the excitation spectrum, a broad excitation peak with many fine structures were observed in the 120–134 nm region and some of their peak positions agreed with Rydberg series I and II given by Tanaka et al.[53] Day et al.[18] measured absorption and fluorescence (190–300 and 190–800 nm) cross sections in a wider excitation wavelength region of 106–152 nm. Absorption and fluorescence cross sections in the 120–135 nm region agreed well with previous data of Okabe.[17]

Figure 8 shows the dependence of 190–300 nm fluorescence cross section on the wavelength in the 121–140 nm (8.86–10.3 eV) region reported by Day et al.,[18] where energies of Kr($^3P_2$), CS(A) + S($^3P_2$) dissociation limit, and eight typical Rydberg states in this wavelength

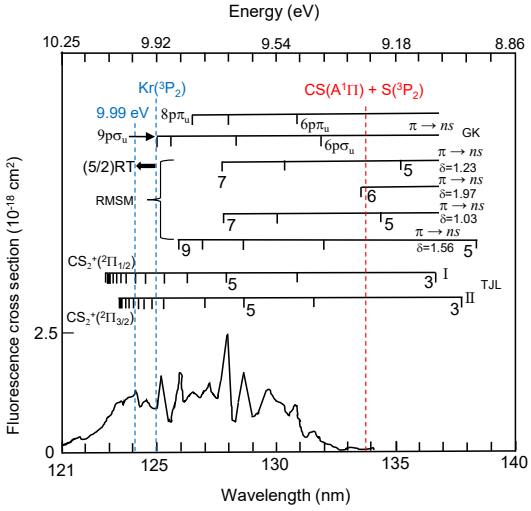

Fig. 8. Dependence of fluorescence cross section of 190–300 nm emission on the wavelength.[18] Rydberg series reported by Tanaka et al. (TJL: Ref. 53), Rabalais et al. (RMSM: Ref. 54), and Greening and King (GK: Ref. 55). Energies of CS($A^1\Pi$) + S($^3P_2$) dissociation limit and Kr($^3P_2$) are also shown.

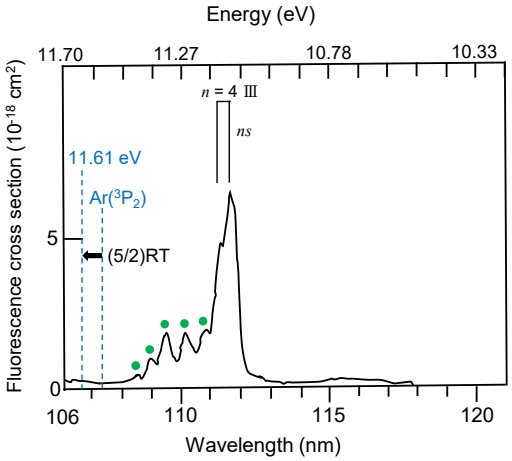

Fig. 9. Dependence of fluorescence cross section of 190–300 nm emission on the wavelength.[18] Green dots are unidentified structures.

region[53-55] are shown. The total energy of reactant Kr($^3P_2$) + CS_2 system is 9.99 eV taking account of (5/2)RT at 300 K. Although many other Rydberg states were identified in this wavelength region,[56-58] they are omitted in Fig. 8 for the sake of clarity. In this wavelength region, many Rydberg series converging to the ground $CS_2^+(\tilde{X}\,^2\Pi_{3/2})$ and $CS_2^+(\tilde{X}\,^2\Pi_{1/2})$ ionic states and those to excited CS_2^+ states are overlapped with each other. Some fluorescence cross-section peaks coincide with such Rydberg states. This indicates that CS(A) is formed through predissociation of Rydberg states in the 121–134 nm (9.25–10.25 eV) region. Since autoionization does not compete with predissociation in Rydberg states below the ionization potential, quantum yield for the production of 190–300 nm fluorescence in the 123–127 nm (9.76–10.07 eV) region is relatively high (≈7%).[18] The near-resonant Rydberg states in the 9.25–9.99 eV region (124–127 nm), especially those in the 9.76–9.99 eV region, will be major precursor CS_2** states in the Kr($^3P_2$)/CS_2 reaction.

Figure 9 shows the dependence of fluorescence cross section on the wavelength in the 106–120 nm (10.3–11.7 eV) region[18] and the energy of Ar($^3P_2$). The total energy of the reactant Ar($^3P_2$) + CS_2 system is 11.61 eV including (5/2)RT at 300 K. In the Ar($^3P_2$)/CS_2 reaction, the most probable precursor states are doublet n = 4 $ns\sigma$-type Rydberg state Ⅲ converging to the $CS_2^+(\tilde{B})$ state and weak features degraded to shorter wavelength region (green dot color bands in Fig. 9). Strong doublet n = 4 Rydberg state Ⅲ bands, which were originally assigned to n = 2 Rydberg state Ⅲ by Tanaka et al.,[53] were revised as n = 4 $ns\sigma$-type Rydberg state Ⅲ by Larzilliere and Damany.[59] Weak additional features in the 108–111 nm region (green dot bands in Fig. 9) were often observed in VUV absorption spectra.[18,53,56,59] These features show a clear vibrational progression having an average spacing of ≈0.065 eV (≈530 cm^{-1}). They are probably associated with autoionization features from various vibrational states of a high lying Rydberg state having a separation close to ν_1 mode.[56] If these features become precursor CS_2** states, excitation of ν_1 mode of CS_2** contributes to vibrational excitation of CS(A) after predissociation to some extent.

In the Ar($^3P_2$)/CS_2 reaction, 0.94 eV is released as rovibrational energies of CS(A), as shown in Table 2. It is therefore highly likely that precursor state is located at least 0.94 eV higher than the CS(A) + S dissociation limit. Such a state with an excitation energy higher than 10.21 eV is higher than the energy of $CS_2^+(\tilde{X})$ (10.07 eV). Therefore, superexcited states above the $CS_2^+(\tilde{X})$ state must be dominantly responsible for the formation of CS(A).

Day et al.[18] reported that the fluorescence cross section of 190–300 nm fluorescence is high in the 109.5–111.5 nm (11.12–11.32 eV) region and its quantum yield is about 3.5%. It is therefore expected that near-resonant

Rydberg states in the 108–113 nm (10.97–11.48 eV) region, especially those in the 11.12−11.32 eV region, will be major precursor states in the $Ar(^3P_2)/CS_2$ reaction. Based on this fact, CS(A) radicals are dominantly formed by predissociation of these superexcited states, where predissociation and autoionization to $CS_2^+(\tilde{X})$ compete with each other.

The above conclusion for the precursor CS_2** states in the $Ar(^3P_2)/CS_2$ reaction is inconsistent with that of Wu.[9] He reported that CS(A) originates from predissociation of the Rydberg state converging into the ground state of CS_2^+ below the ionization limit, via a very steep repulsive potential curve, because fluorescence efficiencies of CS_2 become quite small below the wavelength corresponding to the ionization potential of CS_2 based on the experimental data of Okabe[17] in the 120–135 nm region. However, VUV excitation data by Day et al.[18] in a wider excitation wavelength range of 106–152 nm demonstrated that fluorescence cross section of the 190–300 nm emission has additional peaks in the 108–113 nm region above the $CS_2^+(\tilde{X})$ state (see Fig. 9). We therefore concluded that near-resonant CS_2** states in the 108–113 nm region are more important precursor states than non-resonant Rydberg states in the 121–134 nm region.

De Vries et al.[60] studied the $Ar(^3P_2)/CS_2$ reaction using a beam apparatus. They found that the cross section for dissociative excitation giving CS(A) is largest when the CS_2 bond is perpendicular to the relative velocity vector. According to their proposed reaction dynamics, CS(A) is formed via one or more surface crossings. The most likely formation mechanism is by crossing of entrance V [$Ar(^3P_2)$, CS_2] potential to attractive V (Ar^+, CS_2^-) ion-pair potential followed by another crossing to a high lying V(Ar, CS_2**) neutral potential, which dissociates to Ar + CS_2** Rydberg state. Assuming that the threshold for CS(A:v'= 0) is the same as in photodissociation,[17] the CS(A:v'= 6) level is at 10.02 eV, which is just below the $CS_2^+(\tilde{X})$ level of 10.07 eV. Thus they proposed that CS(A) is formed via crossover from V (Ar^+, CS_2^-) to V(Ar, CS_2**) below the ionization level. As discussed above, the most probable precursor states will be superexcited CS_2** states above the ionization level. Therefore, predissociation of CS_2** Rydberg states below the ionization level will be unimportant for the formation of CS(A) in the $Ar(^3P_2)/CS_2$ reaction.

We proposed the most probable precursor CS_2** Rydberg states in the $Kr(^3P_2)/CS_2$ and $Ar(^3P_2)/CS_2$ reactions. As shown in Fig. 7, the precursor repulsive CS($A^1\Pi$) + S($^3P_2$) curve in the $Kr(^3P_2)/CS_2$ reaction is less steep than that in the $Ar(^3P_2)/CS_2$ reaction. After near-resonant E-E transfer from V [$Kr(^3P_2)$, CS_2] to V(Kr, CS_2**), the V(Kr, CS_2**) potentials cross with the gently repulsive CS($A^1\Pi$) + S($^3P_2$) potential at lower energy region below the ionization level. On the other hand, in the $Ar(^3P_2)/CS_2$ reaction, after similar near-resonant E-E transfer, V(Ar, CS_2**) potentials cross with the highly repulsive CS($A^1\Pi$) + S($^3P_2$) potential at higher energy region above the ionization level. This is a major reason why the $<f_t>$ value in the $Kr(^3P_2)/CS_2$ reaction is smaller than that in the $Ar(^3P_2)/CS_2$ reaction, whereas the $<f_v> + <f_r>$ value in the $Kr(^3P_2)/CS_2$ reaction is higher than that in the $Ar(^3P_2)/CS_2$ reaction.

4. Summary and Conclusion

CS($A^1\Pi$–$X^1\Sigma^+$) emission from v'= 0–5 was observed by the $Kr(^3P_2)/CS_2$ reaction in the FA. The dependence of electronic transition moment on r-centroid was determined from the v'= 1−4 v"-progressions of CS(A−X) emission. The vibrational populations of CS(A:v'= 0–5), $N_{v'}$, and the relative vibrational formation rates of CS(A:v'= 0–5), $P_{v'}$, were estimated. The rotational distribution of CS(A:v'= 0–5) was expressed by single Boltzmann rotational temperatures (T_R) of 1400–2300 K. By using the observed $P_{v'}$ and T_R data, the $<f_v>$, $<f_r>$, and $<f_t>$ values were determined to be 25%, 24%, and 51%, respectively. The observed $P_{v'}$ and T_R data of CS(A:v'= 0–5) were compared with statistical prior vibrational and rotational distributions. The reaction dynamics could not be explained by simple statistical models. It was concluded that major precursor states leading to CS(A) + S($^3P_2$) in the $Kr(^3P_2)/CS_2$ and $Ar(^3P_2)/CS_2$ reactions are near-resonant Rydberg states in the 9.25−9.99 eV and 10.97–11.48 eV region, respectively. Curve crossings between low-energy Rydberg states with gently repulsive CS(A) + S($^3P_2$) curve provide a lower $<f_t>$ value and a higher $<f_v> + <f_r>$ value in the $Kr(^3P_2)/CS_2$ reaction in comparison with those in the $Ar(^3P_2)/CS_2$ reaction.

Acknowledgments

The authors acknowledge Prof. Kenji Furuya of Kyushu University for his careful reading of our manuscript. We would also like to thank

Prof. M. N. R. Ashfold of University of Bristol for sending us a copy of Ref. 16. This work was supported by the Mitsubishi foundation (1996).

References

1) J. A. Coxon, P. J. Marcoux, and D. W. Setser, *Chem. Phys.*, 17, 403 (1976).
2) A. J. Yencha and K. T. Wu, *Chem. Phys.*, 49, 127 (1980).
3) M. Tsuji, H. Obase, M. Matsuo, M. Endoh, and Y. Nishimura, *Chem. Phys.*, 50, 195 (1980).
4) A. Benz, O. Leisin, H. Morgner, H. Seiberle, and J. Stegmaier, *Z. Phys. A, Atoms and Nuclei*, 320, 1123 (1985).
5) M. Tsuji and J. P. Maier, *Chem. Phys.*, 126, 435 (1988).
6) G. W. Taylor, D. W. Setser, and J. A. Coxon, *J. Mol. Spectrosc.*, 44, 108 (1972).
7) G. W. Taylor, *J. Phys. Chem.*, 77, 124 (1973).
8) P. J, Marcoux, M. van Swaay, and D. W. Setser, *J. Phys. Chem.*, 83, 3168 (1979).
9) K. T. Wu, *J. Phys. Chem.*, 89, 4617 (1985).
10) D. Xu, X. Li, G. Shen, L. Wang, H. Chen, and N. Lou, *Chem. Phys. Lett.*, 210, 315 (1993).
11) C. D. Molek, R. Plasil, J. L. McLain, N. G. Adams, and L. M. Babcock, *J. Phys. Chem. A,* 112, 934 (2008).
12) M. T. Jones, T. D. Dreiling, D. W. Setser, and R. N. McDonald, *J. Phys. Chem.*, 89, 4501 (1985).
13) T. A. Carlson, J. Copley, N. Durić, P. Erman, and M. Larsson, *Chem. Phys.*, 42, 81 (1979).
14) J. E. Velazco, J. H. Kolts, and D. W. Setser, *J. Chem. Phys.*, 69, 4357 (1978).
15) L. C. Lee and D. L. Judge, *J. Chem. Phys.,* 63, 2782 (1975).
16) M. N. R. Ashfold, M. Quinton, and J. P. Simon, *J. Chem. Soc., Faraday Trans. 2*, 76, 905 (1980).
17) H. Okabe, *J. Chem. Phys.*, 56, 4381 (1972).
18) R. L. Day, M. Suto, and L. C. Lee, *J. Phys. B, At. Mol. Phys.*, 15, 4403 (1982).
19) M. Tsuji, K. Yamaguchi, S. Yamaguchi, and Y. Nishimura, *Chem. Phys. Lett.*, 143, 482 (1988).
20) G. Herzberg, "*Molecular Spectra and Molecular Structure, I. Spectra of Diatomic Molecules*", Van Nostrand Reinhold, Princeton (1950).
21) P. A. Fraser, *Can. J. Phys.*, 32, 515 (1954).
22) N. Suchard, "*Spectroscopic Constants for Selected Heteronuclear Diatomic Molecules*", Vol. 1 (1975).
23) T. Bergeman and D. Cossart, *J. Mol. Spectrosc.*, 87, 119 (1981).
24) C. A. Mahon, A. Stampanoni, J. Luque, and D. R. Crosley, *J. Mol. Spectrosc.*, 183, 18 (1997).
25) I. Kovács, "*Rotational Structure in the Spectra of Diatomic Molecules*", Hilger, London (1969).
26) D. S. Richards and D. W. Setser, *Chem. Phys. Lett.*, 136, 215 (1987).
27) K. P. Huber and G. Herzberg, "*Molecular Spectra and Molecular Structure, IV. Constants of Diatomic Molecules*", Van Nostrand Reinhold, New York (1979).
28) H. L. Snyder, B. T. Smith, T. P. Parr, and R. M. Martin, *Chem. Phys.*, 65, 397 (1982).
29) *NIST Chemistry WebBook*, NIST Standard Reference Database, Number 69 (2023): http://webbook.nist.gov/chemistry.
30) S. J. Cavanagh, S. T. Gibson, and B. R. Lewis, *J. Chem. Phys.*, 137, 144304 (2012).
31) G. L. Gutsev, R. J. Bartlett, and R. N. Compton, *J. Chem. Phys.*, 108, 6756 (1998).
32) R. D. Levine and J. L. Kinsey, "*Atom-Molecule Collision Theory*", ed. by R. B. Bernstein, Plenum, New York (1979), p. 693.
33) R. B. Bernstein, "*Chemical Dynamics via Molecular Beam and Laser Techniques*", Oxford University Press (1982).
34) R. D. Levine, *Bull. Chem. Soc. Jpn.*, 61, 29 (1988).
35) K. Yamasaki, "*Introduction of Prior Distributions from Statistical Theory*," Isaribi Shoten, (In Japanese), (2023).
36) D. H. Stedman and D. W. Setser, *J. Chem. Phys.,* 52, 3957 (1970).
37) T-D. Nguyen, N. Sadeghi, and J. C. Pebay-Peyroula, *Chem. Phys. Lett.*, 29, 242 (1974).
38) J. H. Kolts, H. C. Brashears, and D. W. Setser, *J. Chem. Phys.,* 67, (1977).
39) T-D. Nguyen and N. Sadeghi, *Chem. Phys.*, 79, 41 (1983).
40) T. Krümpelmann and Ch. Ottinger, *Chem. Phys. Lett.,* 140, 142 (1987).
41) M. Tsuji, K. Yamaguchi, and Y. Nishimura, *Chem. Phys.*, 123, 151 (1988).
42) M. Tsuji, K. Yamaguchi, and Y. Nishimura, *Chem. Phys.*, 125, 337 (1988).
43) M. Tsuji, K. Yamaguchi, H. Obase, and Y. Nishimura, *J. Chem. Phys.*, 90, 5891 (1989).
44) M. Tsuji, K. Yamaguchi, H. Obase, and Y. Nishimura, *Chem. Phys. Lett.*, 161, 41 (1989).
45) E. J. D. Vredenbregt, W. Boom, R. J. F. van Genven, and H. C. W. Beijerinck, *Chem. Phys.*, 145, 267 (1990).
46) M. Tsuji, K. Yamaguchi, H. Kouno, and Y. Nishimura, *Jpn. J. Appl. Phys.*, 30, 1281 (1991).
47) N. Sadeghi, I. Colomb, J. Stoyanova, D. W. Setser, and D. Zhong, *J. Chem. Phys.,* 102, 2744 (1995).
48) Ch. Ottinger, A. F. Vilesov, and D. D. Xu, *Chem. Phys.,* 192, 49 (1995).
49) R. Bachmann, R. Ehlich, Ch. Ottinger, T. Rox, and N. Sadeghi, *J. Phys. Chem. A,* 106, 8328 (2002).
50) W. Böhle, H. Geisen, T. Krümpelmann, and Ch. Ottinger, *Chem. Phys.*, 133, 313 (1989).
51) K. Shuler, *J. Chem. Phys.*, 21, 624 (1953).
52) M.-J. Hubin-Franskin, J. Deiwiche, and P.-M. Guyon, *Z. Phys. D, Atoms Molec. Clusters*, 5, 203 (1987).
53) Y. Tanaka, A. S. Jursa, and F. J. LeBlanc, *J. Chem. Phys.*, 32, 1205 (1960).
54) J. W. Rabalais, J. M. McDonald, V. Scherr, and S. P. McGlynn, *Chem. Rev.*, 71, 73, (1971).
55) F. R. Greening and G. W. King, *J. Mol. Spectrosc.*, 59, 312 (1976).
56) K. Sunanda, A. Shastri, A. K. Das, and B. N. R. Sekhar, *J. Quant. Spectrosc. Radiat. Transf.*, 151, 76 (2015).
57) J.-C. Huang, Y.-S. Cheung, M. Evans, C.-X. Liao, C. Y. Ng, C.-W. Hsu, P. Heimann, H. Lefebvre-Brion, and C. Cossart-Magos, *J. Chem. Phys.,* 106, 864 (1997).
58) C. Cossart-Magos, M. Jungen, and F. Launay, *J. Chem. Phys.,* 109, 6666 (1998).
59) M. Larzilliere and N. Damany, *Can. J. Phys.*, 56, 1150 (1978).
60) M. S. de Vries, G. W. Tyndall, C. L. Cobb, and R. M. Martin, *J. Chem. Phys.,* 86, 2653 (1987).